Metals **2013**, *3*, 202-224; doi:10.3390/met3020202

OPEN ACCESS

metals

ISSN 2075-4701

www.mdpi.com/journal/metals/

Review

Magneto-Structural Properties of Ni_2MnGa Ferromagnetic Shape Memory Alloy in Magnetic Fields

Takuo Sakon [1,*], Yoshiya Adachi [2] and Takeshi Kanomata [3,4]

[1] Department of Mechanical and Systems Engineering, Faculty of Science and Technology, Ryukoku University, Otsu 520-2194, Japan

[2] Graduated School of Science and Engineering, Yamagata University, Yonezawa 992-8510, Japan; E-Mail: adachy@yz.yamagata-u.ac.jp

[3] Research Institute for Engineering and Technology, Tohoku Gakuin University, Tagajo 985-8537, Japan; E-Mail: kanomata@tjcc.tohoku-gakuin.ac.jp

[4] Department of Materials Research, Graduate School of Engineering, Tohoku University, Sendai 980-8579, Japan

* Author to whom correspondence should be addressed; E-Mail: sakon@rins.ryukoku.ac.jp; Tel.: +81-77-543-7443; Fax. : +81-77-543-7457.

Received: 8 March 2013; in revised form: 24 April 2013 / Accepted: 10 May 2013 / Published: 23 May 2013

Abstract: The purpose of this review was to investigate the correlation between magnetism and crystallographic structures as it relates to the martensite transformation of Ni_2MnGa type alloys, which undergo martensite transformation below the Curie temperature. In particular, this paper focused on the physical properties in magnetic fields. Recent researches show that the martensite starting temperature (martensite transformation temperature) T_M and the martensite to austenite transformation temperature (reverse martensite temperature) T_R of Fe, Cu, or Co-doped Ni–Mn–Ga ferromagnetic shape memory alloys increase when compared to Ni_2MnGa. These alloys show large field dependence of the martensite transformation temperature. The field dependence of the martensite transformation temperature, dT_M/dB, is −4.2 K/T in $Ni_{41}Co_9Mn_{32}Ga_{18}$. The results of linear thermal strain and magnetization indicate that a magneto-structural transition occurred at T_M and magnetic field influences the magnetism and also the crystal structures. Magnetocrystalline anisotropy was also determined and compared with other components of Ni_2MnGa type shape memory alloys. In the last section, magnetic field-induced strain and magnetostriction was determined with some novel alloys.

Keywords: ferromagnetic shape memory alloys; magnetocrystalline anisotropy; thermal strain; magnetic field-induced strain; magnetostriction

1. Magnetic Properties of Ni_2MnGa Type Ferromagnetic Shape Memory Alloys

1.1. Outline

Ferromagnetic shape memory alloys (FSMAs) have been extensively studied as potential candidates for smart materials. Among FSMAs, Ni_2MnGa is the most familiar alloy [1]. It has a cubic $L2_1$ Heusler structure (space group $Fm\bar{3}m$) with lattice parameter a = 5.825 Å at room temperature, and it orders ferromagnetically at the Curie temperature $T_C \approx 365$ K [2,3]. Upon cooling from room temperature, a martensite transformation occurs at the martensite transformation temperature $T_M \approx 200$ K. Below T_M, a superstructure is formed because of lattice modulation [4,5]. For the Ni–Mn–Ga Heusler alloys, T_M varies from 200–330 K by non-stoichiometrically changing the concentration of the chemical composition.

Several studies on Ni–Mn–Ga alloys have addressed martensite transformation and correlation between magnetism and crystallographic structures [6–18]. Ma *et al.* [7] studied the crystallography of $Ni_{50+x}Mn_{25}Ga_{25-x}$ alloys (x = 2–11) by powder X-ray diffraction and optical microspectroscopy. In the martensite phase, typical microstructures were observed for $x < 7$. The martensite variants exhibit configurations typical of self-accommodation arrangements. The typical width of a variant is about 1 μm, by means of the TEM image of $Ni_{54}Mn_{25}Ga_{21}$, which is shown in [7], and the strict twin structure of the microstructure is beneficial to the thermoelasticity of its martensitic transformation. A few studies discussed the interaction between magnetism and crystallographic rearrangements [1,8,9,17,18]. The memory strain, which means the second thermal cycle and the relative elongation obtained before the pre-deformation, was observed in single crystal Ni_2MnGa and polycrystal $Ni_{53.6}Mn_{27.1}Ga_{19.3}$ [10]. As for magnetism, the magnetocrystalline anisotropy constant K_U in the martensite phase is 1.17×10^5 J/m^3, which is four times higher than that in the austenite phase (0.27×10^5 J/m^3) [1]. Manosa *et al.* [8] indicated that the martensite transformation takes place in the ferromagnetic phase, and the decrease in magnetization observed at fields between 0 and 1 T is due to the strong magnetocrystalline anisotropy of the martensite phase in association with the multi-domain structure of the martensite state. Sánchez-Alarcos *et al.* [9] investigated the influence of atomic order on the magnetic properties in a polycrystal $Ni_{49.5}Mn_{28.5}Ga_{22}$ ferromagnetic shape memory alloy. Different thermal treatments were performed to modify the degree of the atomic order of the alloy. They analyzed the effect of the different thermal treatments on the magnetic and structural characteristics by a superconducting quantum interference device (SQUID) and differential scanning calorimetry (DSC) measurements. Magnetic and structural properties of the alloys are modified as a consequence of the atomic order change. The martensitic transformation temperatures increase as long as the degree of the atomic order of the alloy increases. On the other side, the Curie temperature and magnetization saturation also reflect the degree of the atomic order of the alloy, but seem to be linked to the particular order of the Mn sub-lattice.

1.2. Magnetocrystalline Anisotropy

Likhachev *et al.* [17] stated that the magnetic driving force responsible for twin boundary motion is practically equal to the magnetocrystalline anisotropy constant K_U. The magnetic driving force applied to twin boundaries is equal to a difference in magnetization free energies between the different twin variants of martensite. This difference also characterizes the energy of uniaxial magnetization anisotropy and can be calculated from the corresponding magnetization measurements. The magnetic driving force achieves its maximal value of 0.13 MPa in a magnetic field higher than 0.8 T. This value is sufficient to explain the high 5% magnetic field-induced strain in some Ni–Mn–Ga alloys, which have very low (2 MPa) twinning stress. They also pointed out that there is a definite analogy between the deformation effects caused by the mechanical and magnetic driving forces. For instance, in both cases, the macroscopic twining strain – driven by the mechanical stress or the magnetic field applied – can be expressed through the same universal function dependent on the corresponding mechanical or magnetic driving force. This universality rule allows performing the quantitative calculations of the magnetic field induced-strain as a function of field by using the mechanical testing results. The magnetization results indicate that the martensite Ni–Mn–Ga alloys have higher magnetocrystalline anisotropy compared to Mn ferrites. Furthermore, magnetization results indicate that the coercivity and saturation field at the martensite phase are higher than those of the cubic austenite phase [11–15]. Zhu *et al.* [11] investigated the lattice constant change $\Delta c/c$ of −4.8% of $Ni_{51.9}Mn_{23.2}Ga_{24.9}$ by means of X-ray diffraction study around martensite transformation temperature. Chernenko *et al.* [12] also studied about magnetization and X-ray powder diffractions, and clear changes were found at T_M for both measurements. Murray *et al.* [18] studied the polycrystal Ni–Mn–Ga alloys. The magnetization step at T_M was also observed, which is a reflection of the magnetocrystalline anisotropy in the tetragonal martensite phase. In the martensite phase, strong magnetocrystalline anisotropy exists. Then the magnetization that reflects the percentage of the magnetic moments parallel to the magnetic field is smaller than that in the austenite phase where the magnetocrystalline anisotropy is not strong in the weak magnetic field. Therefore, the magnetization step is observed at T_M. Nuclear magnetic resonance (NMR) experiment was performed by Golub *et al.* [13] to investigate the correlation between magnetic properties and local structure in Ni–Mn–Ga systems from a microscopic view. NMR experiments indicate Mn-Mn indirect exchange via the faults in Mn-Ga layers interchange caused by excessive Ga. This result indicates that the exchange interaction between Mn-Mn magnetic moments is sensitive with the lattice transformation. Then the magnetism changes from soft magnet in the austenite phase to hard magnet in the martensite phase, which is due to higher magnetocrystalline anisotropy.

To use Ni–Mn–Ga alloys as advanced materials for actuators in daily use, magnetic actuators should be used around room temperature (300 K). Therefore, we selected the $Ni_{52}Mn_{25}Ga_{23}$ alloy, which shows ferromagnetic transition at the Curie temperature T_C (about 360 K), and the martensite transformation occurs around 330 K.

Recently, Sakon *et al.* [19] investigated the correlation between magnetism and crystallographic structures as it relates to the martensite transformation of $Ni_{52}Mn_{25}Ga_{23}$, which undergoes the martensite transformation below T_C [6,7]. The current study particularly focused on the physical properties in magnetic fields. Here, we analyzed that by using the polycrystal samples, it is possible to provide information on the easy axis of the magnetization in the martensite structure with temperature-dependent

strain measurements under the constant magnetic fields. Thermal strain, permeability, and magnetization measurements were performed for polycrystal $Ni_{52}Mn_{25}Ga_{23}$ in magnetic fields (B), and magnetic phase diagrams (B–T phase diagram) were constructed [19]. Thermal strain measurements (linear thermal expansion) and magnetostriction measurements were performed using strain gauges (Kyowa Dengyo Co. Ltd., Chofu, Japan) under steady fields. The magnetic permeability measurements were performed in AC fields with a frequency, f = 73 Hz, and a maximum field, B_{max} = 0.0050 T. AC fields were applied along the longitudinal axis of the sample. Permeability increases above 330 K, and suddenly decreases around 360 K. The temperature dependence of permeability μ and differential of the permeability $d\mu/dT$ are shown in Figure 1a,b, respectively. When cooling from a high temperature, permeability shows a sudden increase at about 356 K and decreases at 327 K. The clear peaks at these temperatures are shown in Figure 1b. The sudden changes in permeability indicate that the ferromagnetic transition occurs around 358 K. The temperature dependence of permeability for $Ni_{52}Mn_{25}Ga_{23}$ is similar to that for $Ni_{52}Mn_{12.5}Fe_{12.5}Ga_{23}$, which shows the transition from a ferromagnetic–martensite (Ferro–M) phase to a ferromagnetic– austenite (Ferro–A) phase [20]. The step around 333 K (heating process) and 327 K (cooling process) for $Ni_{52}Mn_{25}Ga_{23}$ in Figure 1a reflects stronger magnetocrystalline anisotropy in the tetragonal martensite phase [8,18]. Polycrystal $Ni_{49.5}Mn_{28.5}Ga_{22}$, $Ni_{50}Mn_{28}Ga_{22}$ and $Ni_{52}Mn_{12.5}Fe_{12.5}Ga_{23}$ alloys also indicate the magnetization (or permeability) step at T_M [9,18,20] below the field of 10 mT. Figure 2 shows the permeability of $Ni_{52}Mn_{12.5}Fe_{12.5}Ga_{23}$ by means of SQUID magnetometer under the field of 10 mT. After the zero field cooling from room temperature, this measurement was performed. The difference of permeability between increasing temperature and cooling temperature (field cooling) is supposed to the reorientation of the magnetic domains. The permeability of $Ni_{52}Mn_{12.5}Fe_{12.5}Ga_{23}$ also shows abrupt change at T_M = 284 K. The magnetization results are also shown in Figures 3 and 4. As for the temperature dependence of the magnetization (Figure 4), the magnetization at B = 0.5 T, 1 T, and 5 T just above T_M is smaller than that below T_M, which is different from the temperature dependence of the permeability in Figure 2. It is conceivable that the magnetocrystalline anisotropy in the martensite phase is larger than that in the austenite phase. As for $Ni_{49.5}Mn_{28.5}Ga_{22}$ [9], the permeability measurement results indicate that the ferromagnetic transition from the paramagnetic–austenite (Para–A) phase to the Ferro–A phase occurs around 358 K. On the other hand, for $Ni_{52}Mn_{25}Ga_{23}$, the linear strain does not show noticeable anomaly at the ferromagnetic transition around 358 K (Figure 5). When cooling from 370 K, the thermal strain shows a peak at 329 K for $Ni_{52}Mn_{25}Ga_{23}$. This may be attributed to the intermingling of the $L2_1$ austenite lattices and the *14M* martensite lattices at the martensite transformation. The sequential phenomenon is observed in single crystal $Ni_{2.19}Mn_{0.81}Ga$ [21]. Zhu *et al.* [11] suggest that the small satellite peaks in heat flow plot of $Ni_{51.9}Mn_{23.2}Ga_{24.9}$, which flanks the central peak, indicate that the structural transition takes place in multiple steps. The results of thermal strain in a magnetic field and magnetic field-induced strain yield information about the twin boundary motion in the fields.

Figure 1. (**a**) Temperature dependence of the permeability of $Ni_{52}Mn_{25}Ga_{23}$. (**b**) Temperature dependence of the differential of the permeability.

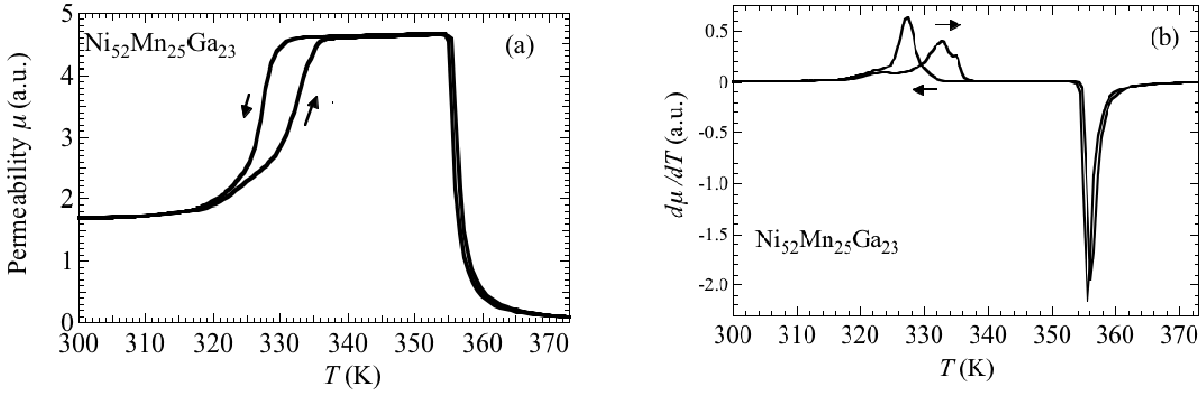

Figure 2. The temperature dependence of the permeability of $Ni_{52}Mn_{12.5}Fe_{12.5}Ga_{23}$.

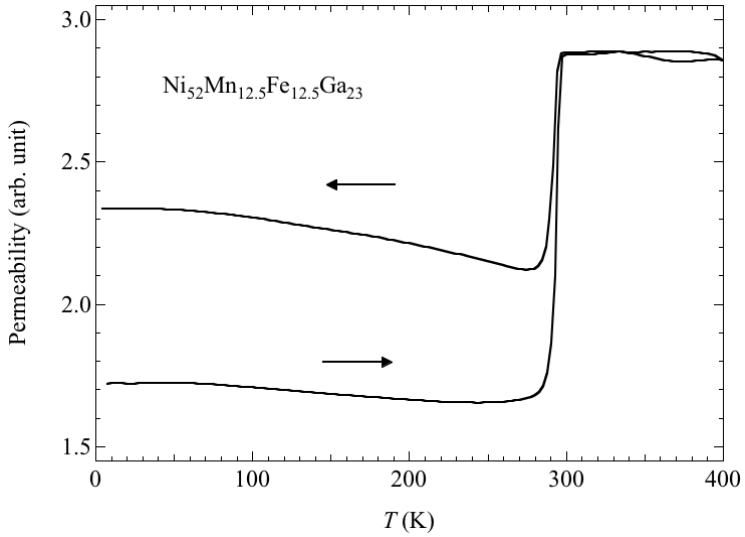

Figure 3. The magnetic field dependence of the magnetization of $Ni_{52}Mn_{12.5}Fe_{12.5}Ga_{23}$.

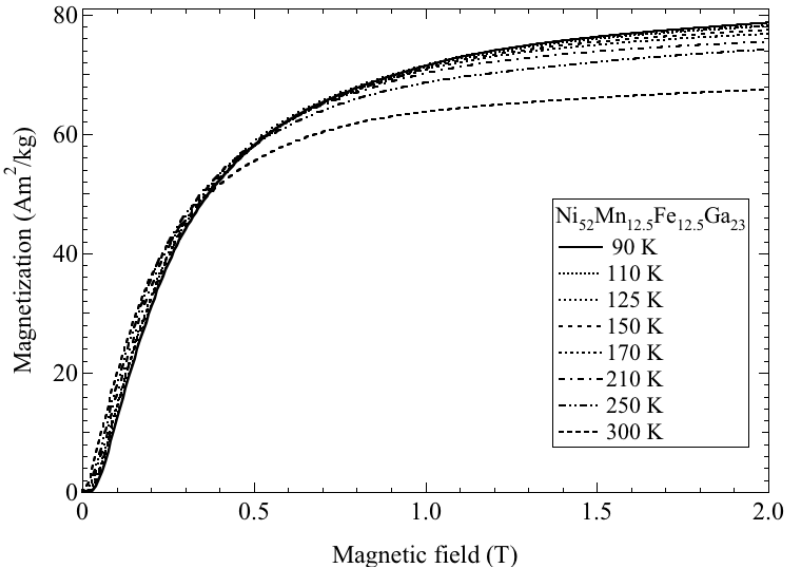

Figure 4. The temperature dependence of the magnetization of $Ni_{52}Mn_{12.5}Fe_{12.5}Ga_{23}$.

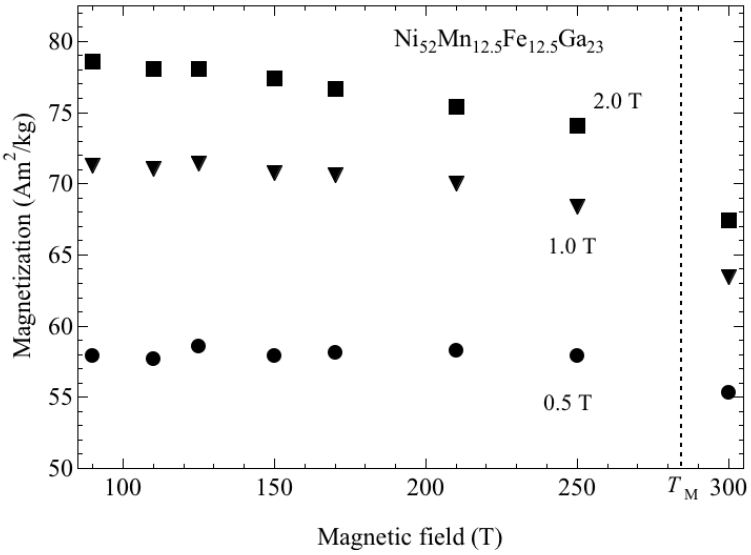

Figure 5. The linear thermal strain of $Ni_{52}Mn_{25}Ga_{23}$ along the applied magnetic fields.

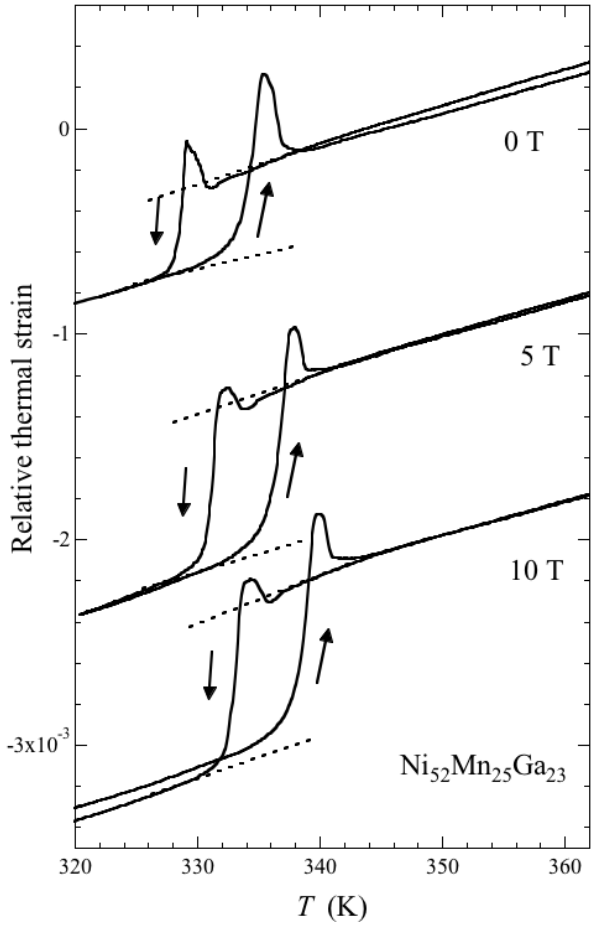

The difference of magnetocrystalline anisotropy constant K_U between the value in the martensite phase and that in the austenite phase for a Ni_2MnGa single crystal [1] indicates that the magnetocrystalline anisotropy is about four times larger in the martensite phase than the austenite phase. The Zeeman energy and/or magnetocrystalline anisotropy energy that is sufficient to induce motion of

the twin boundary is denoted as $M_S B_S/2 = K_U$ [1], where, M_S is the saturated magnetization and B_S is the saturated magnetic field. Kim *et al.* [14] also mentioned that the magnetocrystalline anisotropy energy is of the order of 10^5 J/m^3. From the permeability and magnetization measurements, the magnetocrystalline anisotropy constant K_U of $Ni_{52}Mn_{25}Ga_{23}$ can be calculated [19]. Spontaneous magnetization is provided from the value that M^2 intersects the y-axis in the Arrott plot (M^2 *vs.* B/M plot) in order to obtain a spontaneous magnetization. Spontaneous magnetization in $Ni_{52}Mn_{25}Ga_{23}$ at 333 K, just below T_R, is 42.2 Am^2/kg (=emu/g), which was obtained by the Arrott plot. When using this value as M_S, the magnetocrystalline anisotropy energy in the martensite phase of $Ni_{52}Mn_{25}Ga_{23}$ is $M_S B_S/2 = K_U = 1.04 \times 10^5$ J/m^3, which is in the same order as the martensite phase of Ni_2MnGa. These magnetic properties were also shown for $Ni_{51.9}Mn_{23.2}Ga_{24.9}$ [11], $Ni_{49.7}Mn_{29.1}Ga_{21.2}$ [12], and $Ni_{54}Mn_{21}Ga_{25}$ [13]. These results are indicative of high magnetocrystalline anisotropy.

Straka *et al.* [22] performed a study on temperature dependence of magnetocrystalline anisotropy of three different martensites known to exist in the Ni–Mn–Ga alloys. The anisotropy constants were determined from magnetization curves measured at different temperatures. The anisotropy of $Ni_{50.5}Mn_{29.4}Ga_{20.1}$ five-layered modulated tetragonal martensite single crystal is uniaxial with easy magnetization direction along the short crystallographic axis. At room temperature, K_1 (rt) = 1.65×10^5 J/m^3 and K_2 is negligible, where coefficients K_1 and K_2 are correspondingly the first- and second-order anisotropy constants. $Ni_{50.5}Mn_{29.4}Ga_{21.2}$ seven-layered modulated orthorhombic martensite single crystal exhibits easy magnetization direction along the shortest crystallographic axis. K_1 (rt) = 1.7×10^5 J/m^3 and K_2 (rt) = 0.9×10^5 J/m^3 referring to hard and mid-hard magnetization axes. Nonmodulated tetragonal martensite possesses a uniaxial anisotropy with easy plane and hard magnetization direction along the long crystallographic axis with $K_1 = -2.3 \times 10^5$ J/m^3 and $K_2 = 0.55 \times 10^5$ J/m^3 at room temperature. For uniaxial anisotropy, the temperature dependence of the first anisotropy constant K_1 below T_c can be described by magnetization power law [23,24]:

$$K_1(T)/K_1(0) = [M_s(T)/M_s(0)]^n \quad (1)$$

where, M_s is the saturation magnetization. Co follows this power law with exponent $n = 3$. Fe follows with exponent $n = 4$ [25].

The temperature dependence of K_1 (T) follows magnetization power law with exponent $n = 3$ in Equation (1) suggesting a single ion origin of the magnetocrystalline anisotropy in Ni–Mn–Ga marten site. The temperature dependence of K_1 and K_2 does not follow power law with exponent $n = 3$; rather n is between two and three.

Okamoto *et al.* [26] measured the magnetizations of *10 M* martensite in Ni_2MnGa and *2 M* martensite in $Ni_{2.14}Mn_{0.92}Ga_{0.94}$ single crystals. As for Ni_2MnGa, the magnetic easy axis is the *c* axis. On the contrary, the magnetic easy axis is the *a* axis for $Ni_{2.14}Mn_{0.92}Ga_{0.94}$. Magnetocrystalline anisotropy constant (K_u) of Ni_2MnGa and $Ni_{2.14}Mn_{0.92}Ga_{0.94}$ is 5.9×10^5 J/m^3 and 4.3×10^5 J/m^3, respectively. Concerning the magnetization power law, Equation (1), for Ni_2MnGa and $Ni_{2.14}Mn_{0.92}Ga_{0.94}$, it follows power law with exponent $n = 3$. The difference of the K_u between the Ni_2MnGa alloys is presumed that the variant types in the martensite phase are different with each other.

The magnetocrystalline anisotropy of nonmodulated Ni–Mn–Ga alloy was investigated by Heczko *et al.* [27]. Five-layered modulated nearly tetragonal *5 M* with $c < a = b$, seven layered orthorhombic 7 *M* with $c < b < a$, and nonmodulated (NM) tetragonal phases with $c > a = b$. The

absolute value of anisotropy constant of NM $Ni_{50.5}Mn_{30.4}Ga_{19.1}$ single crystal increases from 2.6×10^5 J/m^3 at 300 K to 5×10^5 J/m^3 at 10 K under the tensile stress of 40 MPa. The obtained exponent in power law of Equation (1) is $n = 2.5$.

Now we compare the Ni–Mn–Ga alloys with 4*f* rare earth compounds and 5*f* uranium compounds, which have a highly magnetocrystalline anisotropy. The magnetization of Nd_2Fe_{17} single crystal indicates that the *c*-axis is the hard axis and the *b*-axis is the easy one [28]. The magnetocrystalline anisotropy constants of the Nd-sublattice were estimated to be $K_1^{Nd} = -5.7 \times 10^7$ J/m^{3}and $K_2^{Nd} = 2.6 \times 10^7$ J/m^3. The temperature dependence of the second order magnetocrystalline anisotropy constant K_2° in Equation (1) strayed out from the curve of power law with $n = 3$. The saturation magnetization is mainly dominated by the Fe-sublattice moment, where the magnetocrystalline anisotropy is strongly dominated by the Nd-sublattice anisotropy. The sharp drop of the anisotropy constant K_2° is mainly due to the large thermal fluctuation of the magnetic moment of theNd-sublattice with temperature, compared with the Fe-sublattice.

As for 5*f* electron compound UGe_2 single crystal [29], it has a highly magnetocrystalline anisotropy because the magnetization curves reflect the large magnetocrystalline anisotropy. The magnetocrystalline anisotropy constant $K_1 = 3.4$ kJ/kg. The density value $\rho = 10.26$ g/cm^3 = 1.026×10^4 kg/m^3 [30]. Then $K_1 = 3.4 \times 10^3$ J/kg × 1.026×10^4 kg/m^3 = 3.5×10^7 J/m^3. This value is comparable with that of K_1^{Nd} for Nd_2Fe_{17} single crystal. The exponent n in Equation (1) is 1. This is smaller than $n = 3$. This analysis indicates that UGe_2 retains magnetocrystalline anisotropy until high temperature.

Table 1. Magnetocrystalline anisotropy constant *K* and temperature dependence of *K*.

Sample	Structural phase	K(10^4 J/m^3)	Exponent n in Equation (1)	Remarks
Fe	Bcc	4.8	4	[24]
Co	Hcp	45	3	[24]
αFe_2O_3 (hematite)	($\bar{3}2$/m)	120		[24]
Ni_2MnGa	Martensite	11.7		single crystal [1]
Ni_2MnGa	$L2_1$austenite	2.7		single crystal [1]
Ni_2MnGa	10M martensite	59	3	single crystal [26]
$Ni_{2.14}Mn_{0.92}Ga_{0.94}$	2M martensite	43	3	single crystal [26]
$Ni_{52}Mn_{25}Ga_{23}$	14M martensite	10.4		polycrystal [19]
$Ni_{50.5}Mn_{30.4}Ga_{19.1}$	NM martensite	26 (300 K) 50 (10K)	2.5	single crystal 40 MPa tensile stress [27]
$Ni_{50.5}Mn_{29.4}Ga_{20.1}$	5M martensite	K_1 16.5 K_2 negligible	2~3	single crystal room temp. [22]
$Ni_{50.5}Mn_{29.4}Ga_{21.2}$	7M martensite	$K_1$17 $K_2$9	2~3	single crystal room temp. [22]
Nd_2Fe_{17}	Rhombohedral Th_2Zn_{17}	$K_1^{Nd} = -5700$ $K_2^{Nd} = 2600$	Stray out from Equation (1)	single crystal 4.2 K [28]
UGe_2	Orthorhombic C_{mmm} $ThGe_2$	3500	1	single crystal 4.2 K [29]

Magnetocrystalline anisotropy constant *K* and the exponent of Equation (1) are summarized in Table 1. With an increase in constant *K*, the exponent *n* comes smaller. In strong correlated electron

systems such as 4*f* or 5*f* electron compounds, which have highly anisotropic electron orbital, itinerant bands predominate the magnetic properties.

In the next section, we mention the theoretical studies about the phase diagram of Ni_2MnGa type Heusler alloys considering the magnetocrystalline anisotropy [31].

2. Structural and Magnetic Properties in Magnetic Fields

In this section, we mention the substitution Fe, Cu, or Co atoms for Mn or Ga atoms in Ni_2MnGa alloys.

Ni-Fe-Ga Heusler alloys are the new promising FSMAs for which T_M varies from 150 K to room temperature and exhibits excellent ductility [32–34]. The $Ni_{54}Fe_{19}Ga_{27}$ alloy transforms from high temperature $L2_1$ phase to the martensite phase having a monoclinic structure [33,34]. Kikuchi *et al.* [20] have reported the magnetic properties of $Ni_{50+x}Mn_{12.5}Fe_{12.5}Ga_{25-x}$ ($0 \leq x \leq 5.5$) ferromagnetic alloys, which were produced by replacing Ga with Ni in $Ni_{50}Mn_{12.5}Fe_{12.5}Ga_{25}$ alloy. The measurements of temperature dependence of magnetization for this series were performed [35]. It was observed that T_C gradually decreases with the concentration x, while T_M and the reverse martensitic transformation temperature T_R increases with x and exhibits saturation behavior for $x \geq 3.0$. The linear thermal expansion measurements of $Ni_{52}Mn_{12.5}Fe_{12.5}Ga_{23}$ were performed in static magnetic fields. When cooling from 310 K (Ferro-A phase), the alloy shrinks gradually in zero magnetic fields. Small elongation was observed at 288 K. Then, sudden shrinking occurs below 286 K, which indicates transformation from the austenite to martensite phase. The T_M of this alloy is 284 K. The reason of small elongation at 288 K is considered to be that $L2_1$ and *14M* structures coexist each other. Therefore, apertures between $L2_1$ and *14M* structures were originated and a small expansion occurred. As for $Ni_{2+x}Mn_{1-x}Ga$ alloys, small elongation was observed just above T_M [36]. The phase below T_M is Ferro-M. When heating from 270 K, expansion occurs at about T_R = 288 K, which indicates reverse martensitic transformation [20]. Small elongations just above the temperatures of T_M and T_R were also observed in polycrystal $Ni_{2+x}Mn_{1-x}Ga$ ($0.16 \leq x \leq 0.20$) [36].

T_M and T_R gradually changed with increasing magnetic fields. The strain at T_M and T_R was about -2.5×10^{-3} (−0.25%) and was almost the same as that in magnetic fields. Kikuchi *et al.* [20] performed the X-ray diffraction experiments of $Ni_{50+x}Mn_{12.5}Fe_{12.5}Ga_{25-x}$. The X-ray patterns at room temperature (T = 300 K, austenite phase) for the samples of $0 \leq x \leq 2.0$ were indexed with the $L2_1$ Heusler structure. In the X-ray diffraction pattern at room temperature of the sample with x = 2.0, a very weak reflection from a γ phase was observed, where the γ phase has a disordered face-centered cubic (fcc) structure. The lattice parameter a of x = 2.0 was found to be 5.7927 Å [37]. On the other hand, the martensite phase appeared at room temperature. The martensitic structure of x = 3.0 was indexed as a monoclinic structure with *14 M* (*7R*) structure. The lattice parameters of the sample were determined as a = 4.2495 Å, b = 2.7211 Å, c = 29.340 Å, and β = 93.36° at room temperature. We estimated the strain of $Ni_{52}Mn_{12.5}Fe_{12.5}Ga_{23}$ (x = 2.0) at T_M using the lattice parameter of x = 2.0 in the austenite phase and x = 3.0 in the martensite phase [35]. In the austenite phase, for the $L2_1$ cubic structure, the lattice parameter a was 5.7927 Å. The distance between Mn–Mn atoms was $a/\sqrt{2}$ = 4.0961 Å, and the volume of the unit cell was $V_A = (a/\sqrt{2})^3 = (4.0961)^3 = 68.72$ Å^3. Furthermore, the volume V_M in the martensite phase was estimated and compared with V_A in the same area. In the *14 M* (*7R*) martensite

phase, a = 4.2495 Å in the basal plane is parallel to one of the a axis in the $L2_1$ structure, and is of the same unit. The other axis in the martensite phase corresponds to one of the a axis in the $L2_1$ structure of the Mn–Mn ridge in the basal plane ($\sqrt{2} \times b$). The c axis is almost normal ($\beta = 93.36°$) to the basal plane and the seven Mn–Mn cycles at c = 29.340 Å. Therefore, the volume,

$$V_M = a \times (c/7) \times (\sqrt{2} \times b) \times \sin\beta = 4.2495 \times 4.1914 \times (1.4142 \times 2.7211) \times \sin 93.36° = 68.55 \times 0.9983 = 68.43 \text{ Å}^3 \quad (2)$$

The linear strain of a polycrystal is one-third of the volume strain. Therefore, we estimate the linear strain $\Delta\varepsilon$ as,

$$\Delta\varepsilon = \{(V_M - V_A)/V_A\} \times 1/3 = \{(68.43 - 68.72)/68.72\} \times 1/3 = (-0.29/68.72) \times 1/3 = -0.14\% \quad (3)$$

This estimated value is approximately comparable to the strain value $\Delta\varepsilon = -0.25\%$ of $Ni_{52}Mn_{12.5}Fe_{12.5}Ga_{23}$ obtained from the experimental study in [35].

T_M and T_R gradually changed with increasing magnetic fields. The strain at T_M and T_R was about -2.5×10^{-3} (−0.25%) and was almost the same as that in magnetic fields. For $Ni_{52}Mn_{12.5}Fe_{12.5}Ga_{23}$, the shifts of T_M in magnetic fields (B) were estimated as $dT_M/dB \approx 0.5$ K/T from the thermal strain measurement results in magnetic fields. The shifts of T_M indicate that magnetization influences martensite transformation and the increase of T_M in accordance with the magnetic fields is proportional to the difference between the magnetization of the austenite phase with that of the martensitic phase.

Kataoka *et al.* [31] have reported the magnetic properties of $Ni_2Mn_{1-x}Cu_xGa$ ($0 \le x \le 0.40$) alloys, which were obtained by replacing Mn with Cu in Ni_2MnGa alloy. The samples with $0.23 \le x \le 0.30$ show martensite transformation at about 300 K. The magnetic and crystal states above and below T_M are the paramagnetic austenite phase (Para-A), and the ferromagnetic martensite phase (Ferro-M), respectively. Such Heusler alloys show martensitic transformation around room temperature. The temperature dependence of magnetic permeability and linear thermal expansion of $Ni_2Mn_{0.75}Cu_{0.25}Ga$ in zero magnetic fields, were performed [35]. When cooling from a high temperature in the parent austenite phase, it shrinks and the permeability increases at about T_M = 308 K. The permeability at the austenite phase is very low compared to the martensite phase. These results indicate that the region above T_M or T_R is Para-A and the region below T_M or T_R is Ferro-M. When heating from a low temperature, the expansion occurs at about T_R = 316 K, which indicates reverse martensitic transformation. The strain at T_M or T_R is about 3.0×10^{-3} (0.30%). Kataoka *et al.* [31] studied the X-ray powder diffraction of $Ni_2Mn_{1-x}Cu_xGa$ ($0 \le x \le 0.40$). The X-ray diffraction measurement of $Ni_2Mn_{0.75}Cu_{0.25}Ga$ indicates that the austenite phase is cubic $L2_1$ phase and the martensite phase is *14 M* phase. From the temperature dependence of the linear thermal expansion of $Ni_2Mn_{0.75}Cu_{0.25}Ga$ in static magnetic fields, it was revealed that T_M and T_R gradually changed with increasing magnetic fields. The shifts of T_M in magnetic fields (B) were estimated as dT_M/dB = 1.2 K/T. The value is twice larger than that of $Ni_{52}Mn_{12.5}Fe_{12.5}Ga_{23}$, which is mentioned above. The reason is that, for $Ni_{52}Mn_{12.5}Fe_{12.5}Ga_{23}$, martensite transformation occurred in a ferromagnetic phase. On the contrary, magnetic transition and structural transition (martensite transformation) occurred at the same temperature. Magneto-structural phase transition largely influences the shifts of T_M in magnetic fields.

Thermal expansion, permeability, and magnetization measurements of ferromagnetic shape memory alloy, $Ni_2MnGa_{0.88}Cu_{0.12}$, were performed across T_M and T_R at atmospheric pressure [38]. When cooling from the austenite phase, a steep decrease was found in thermal expansion due to martensite transformation. The permeability indicates a sharp peak around T_M and ferromagnetism below T_M. Considering the permeability and magnetization results of $Ni_2MnGa_{0.88}Cu_{0.12}$, the region above T_M or T_R is the Para-A phase and the region below T_M or T_R is the Ferro-M phase. T_M and T_R increased gradually with increasing magnetic field. The shift of T_M in magnetic fields around zero magnetic fields were estimated as dT_M/dB = 1.3 K/T. The shift of T_M also indicates that magnetization influences martensite transformation and the increase of T_M in accordance with the magnetic fields is proportional to the difference between the magnetization of austenite and martensite phases.

Albertini *et al.* [39] investigated the composition dependence of the structural and magnetic properties of the Co-doped Ni–Mn–Ga ferromagnetic shape memory alloy around the Mn-rich composition $Ni_{50}Mn_{30}Ga_{20}$. The magnetic and structural properties displayed noticeable discontinuities across the martensite transformation; there was a remarkable jump (ΔM) in the values of the saturation magnetization at the transformation, which indicates that a metamagnetic transition occurred under the magnetic field. The field dependence of the martensite transformation temperature (dT_M/dB) and that of the crystalline volume change ($\Delta V/V$) was reported and found to be considerably enhanced by the additional In-doping of the quaternary alloy. The most remarkable alloy is $Ni_{41}Co_9Mn_{32}Ga_{18}$ [39]. When cooling from 500 K, it shows a ferromagnetic transition at T_C^A = 456 K in the austenite phase. At the martensite transformation temperature, T_M = 420 K, its AC susceptibility drastically decreased. Below 300 K, its AC susceptibility gradually increased and a distinct peak was found at T_C^M = 257 K in the martensitic phase. When heating from 200 K, the Curie temperatures T_C^M and T_C^A were the same as the temperatures in the cooling process. The reverse martensitic temperature T_R was 436 K. Thus, AC susceptibility indicates re-entrant magnetism, ferromagnetic-paramagnetic, or weak ferromagnetic-ferromagnetic states, which may be related to the crystal structures. Thermal strain, magnetostriction, and magnetization measurements of the polycrystal ferromagnetic shape memory alloy, $Ni_{41}Co_9Mn_{31.5}Ga_{18.5}$, were performed across T_M and T_R, at atmospheric pressure [40]. The AC susceptibility also indicates re-entrant magnetism. The isothermal magnetization curve (*M vs. B*) shows S-shape metamagnetic transition between 320 K and 390 K. Strong magneto-structural coupling was indicated by the magnetic properties and phase transitions. When cooling from the austenite phase, a steep decrease in the thermal expansion due to the martensite transformation at T_M was found. When heating from the martensitic phase, a steep increase in the thermal expansion due to the reverse martensite transformation at T_R was observed. These transition temperatures decreased gradually with increasing magnetic field. The field dependence of the martensite transformation temperature, dT_M/dB, is −4.2 K/T and that of the reverse martensite transformation temperature, dT_R/dB, is −7.9 K/T in $Ni_{41}Co_9Mn_{31.5}Ga_{18.5}$. The metamagnetic transition appeared between 330 K and 390 K. The results of thermal strain and magnetization indicate that a magneto-structural transition occurred at T_M. $Ni_{50-x}Co_xMn_{31.5}Ga_{18.5}$ ($0 \leq x \leq 9$) was also investigated across the martensite transformation temperature T_M and the reverse martensite transformation temperature T_R at atmospheric pressure [41]. By means of X-ray powder diffraction, the samples were confirmed as a single phase with $D0_{22}$ tetragonal structure at 298 K in the martensite phase. These transition temperatures increased gradually with increasing Co component x. Moreover, temperature hysteresis in the thermal cycles of the

magnetization across the T_R and T_M became larger with the increasing of x. Wide temperature hysteresis of $T_M - T_R = -65$ K at zero fields was observed in the thermal strain measurement.

Table 2. Spontaneous magnetization and dT_M/dB in Heusler Ni_2MnGa type magnetic shape memory alloys. M_M and M_A indicate the spontaneous magnetizations in the martensite phase and austenite phase, respectively. Ferro and Para mean the ferromagnetic and the paramagnetic phases, respectively. T_C^M indicates the Curie temperature in the martensite phase, and T_C^A indicates the Curie temperature in the austenite phase.

Sample	M_M	M_A	$(M_M - M_A)/M_M$	dT_M/dB(K/T)	Remarks
Ni_2MnGa	90 Am^2/kg at 180 K (*1) Ferro	80 Am^2/kg at 220 K (*1) Ferro	0.11	0.20 (*2) 0.40 ± 0.25 (*3)	*1 [2] *2 [25] *3 [26]
$Ni_{2.19}Mn_{0.81}Ga$	2.0 (a.u.) (*4) at 300 K Ferro	0 (a.u.) (*4) at 350 K Para	1.0	1.0 (*4)	*4 [28]
$Ni_{52}Mn_{12.5}Fe_{12.5}Ga_{23}$	63.1 Am^2/kg at 250 K Ferro	52.7 Am^2/kg at 300 K Ferro	0.16	0.5	[20]
$Ni_2Mn_{0.75}Cu_{0.25}Ga$	42.4 Am^2/kg at 300 K Ferro	0 Am^2/kg at 307 K Para	1.0	1.2	[20]
$Ni_2MnGa_{0.88}Cu_{0.12}$	37.3 Am^2/kg at 330 K Ferro	0 Am^2/kg at 340 K Para	1.0	1.3	[29]
$Ni_{52}Mn_{25}Ga_{23}$	42.2 Am^2/kg at 333 K Ferro	34.2 Am^2/kg at 335 K Ferro	0.19	0.43	[19]
$Ni_{45}Co_5Mn_{36.7}In_{13.3}$	0 Am^2/kg at 270 K Para	70 Am^2/kg at 320 K Ferro	−1.0	−4.3	[42]
$Ni_{43}Co_7Mn_{31}Ga_{19}$	20 Am^2/kg at $T_C^M \leq T \leq T_M$ Para or weak Ferro	59.2 Am^2/kg at $T_M \leq T \leq T_C^A$ Ferro	−0.64	−2.95	[39]
$Ni_{41}Co_9Mn_{32}Ga_{18}$	4.0 Am^2/kg at $T_C^M \leq T \leq T_M$ Para or weak Ferro	53.3 Am^2/kg at $T_M \leq T \leq T_C^A$ Ferro	−0.92	−2.8	[39]
$Ni_{41}Co_9Mn_{31.5}Ga_{18.5}$	12 Am^2/kg at $T_C^M \leq T = 316$ K $\leq T_M$ Para or weak Ferro	79 Am^2/kg at $T_M \leq T = 388$ K $\leq T_C^A$ Ferro	−0.84	−4.2	[40]

Single crystal $Ni_{45}Co_5Mn_{36.7}In_{13.3}$ (13.3 In), which was studied by Kainuma *et al.* [42], also shows the re-entrant ferromagnetic property. The T_M and T_R decreased with the increasing of magnetic fields. The thermo-magnetization curve (*M vs. T*) indicates that the decrease of T_M, ΔT_M from 0.05 T to 7.0 T is about 30 K. Large hysteresis was shown in the thermo-magnetization curve. Monroe *et al.* [43] suggested that Kinetic Arrest effect phenomenon appeared in Ni-Co-Mn-In alloys. The magnetic field change of the T_M, dT_M/dB, is −4.3 K/T. The isothermal magnetization curve (*M vs. B*) shows S-shape metamagnetic transition between 270 K and 310 K [42,44].

Spontaneous magnetizations at the martensite phase M_M and the austenite phase M_A are shown in Table 2. The dT_M/dB is also shown. It is clear that the dT_M/dB of the alloys of which magnetic transition

and martensite transiton occurs at almost the same temperature are large. Some Ni-Co-Mn-Ga and Ni-Co-Mn-In alloys indicate minus dT_M/dB values, which indicate the re-entrant magnetism. These results indicate that the magneto-structural interactions are large in the alloys, which have large dT_M/dB values.

The change in transition temperature (ΔT) induced by a change in magnetic field (ΔB) is approximately given by the Clausius–Clapeyron relation in the magnetic phase diagram as

$$\frac{\Delta B}{\Delta T} \approx \frac{dB}{dT} = -\frac{\Delta S}{\Delta M} \tag{4}$$

where ΔM and ΔS are the differences in magnetization and entropy change between the austenite and martensitic phases, respectively [42,45]. From the experimental results in this study, dT_R/dB is determined as −7.9 K/T in $Ni_{41}Co_9Mn_{32}Ga_{18}$. Therefore, dB/dT_R is −0.13 T/K. The entropy change, ΔS, obtained from the DSC measurement is 7.3 J/kg K. From the magnetization results, ΔM is 40 Am^2/kg, and then, $-\Delta S/\Delta M = dB/dT$ is −0.18 T/K, given by Equation (2). However, the measured dT_R/dB = −0.13 K/T is 30% smaller than the calculated value. The latent heat of the martensite transformation is not small. Therefore, the ambiguity for the value of ΔS is large, thereby giving rise to the large ambiguity present in this calculation.

Satyanarayan *et al.* [46] and Nishiyama [47] mentioned the relation between free energy and T_M or T_R in magnetic fields. It is well known that the T_M of Iron steels increase with increasing magnetic fields. The dT_M/dB is about few K/T. The increase of the martensite α' phase is a few percent for 1 T field increase. In usual Iron steels, γ phase is the nonmagnetic phase and α' phase is the ferromagnetic phase.

The free energy of α' phase is lower in magnetic fields and then, the percentage of α' phase increases. This is because the free energy lowers due to Zeeman energy in ferromagnetic α' phase. Figure 6 shows the temperature and magnetic field dependence of Gibbs's free energy. In zero fields, the martensite transformation occurs at the T_M, where the motive force ΔF is equal to the difference of the free energy between the martensite α' phase and γ phase. In magnetic fields, the free energy of α' phase is lowered due to the Zeeman energy magnetic energy ΔE. Consequently, the T_M increases, as shown in Figure 6(a). The relation between ΔF, ΔE, T_M, and ΔT, the temperature change of T_M, is,

$$\Delta T = \frac{\Delta E}{\Delta F}(T_0 - T_M) \tag{5}$$

where, $T_0 = \frac{T_M + T_R}{2}$.

In some Iron steels, experimental results and calculated results obtained by Equation (3) are almost the same [46]. This approach could be applicable to ferromagnetic Heusler alloys Ni_2MnGa and $Ni_{2+x}Mn_{1-x}Ga$.

Meanwhile, the T_M of Ni-Co-Mn-Ga and Ni-Co-Mn-In alloys decreases with increasing magnetic fields, as shown in Figure 6(b). The phase just below the T_M of these alloys is the martensite paramagnetic (or weak ferromagnetic) phase and the phase just above the T_M is the ferromagnetic austenite phase. In magnetic fields, the free energy of the austenite phase lowers and the percentage of the austenite increases due to Zeeman energy. Consequently, in the magnetic *B*-*T* phase diagram, the domain of the austenite phase increases and the T_M decreases.

Figure 6. Temperature and magnetic field dependence of Gibbs's free energy. (**a**) The diagram when the martensite phase is ferromagnetic and the austenite phase is paramagnetic. ΔF and ΔE indicate the motive force for inducing a martensite transition, and the Zeeman energy, respectively. Dashed bold line indicates the free energy under the magnetic field at the martensite phase. (**b**) The diagram when the martensite phase is paramagnetic and the austenite phase is ferromagnetic. Dashed bold line indicates the free energy under the magnetic field at the austenite phase.

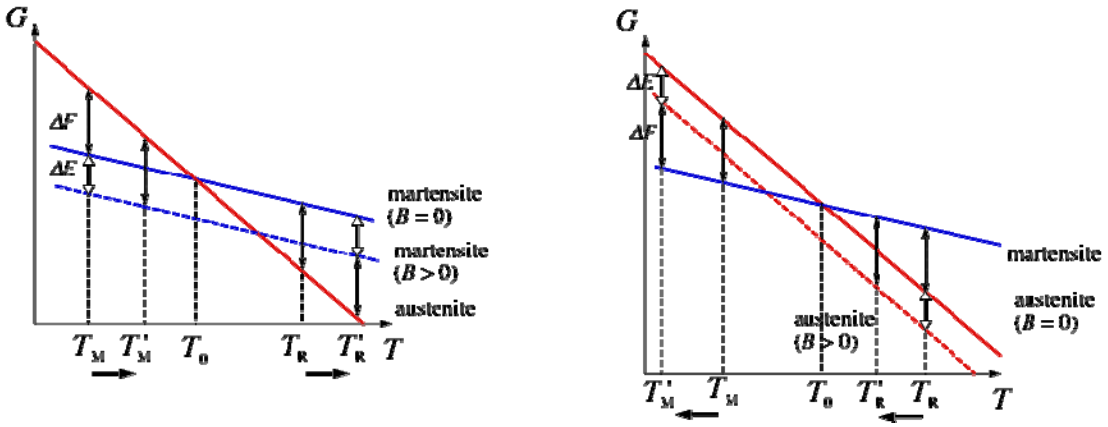

Now we apply Equation (3) to $Ni_{41}Co_9Mn_{32}Ga_{18}$. T_M = 315 K, T_R = 380 K, T_o = 348 K at zero fields. $\Delta T = T_o - T_M$ = 33 K. $\Delta E_m = MB$ = 100 J/kgT (at 8 T) × 8 T = 800 J/kg. [J/kg] = [emu/g] = [Am^2/kg]. From the DSC measurement, ΔF = 1.0 kJ/kg. Then, $\Delta T = \frac{800}{1{,}000} \times 33 = 26$ K for ΔB = 8 T. $\Delta T/\Delta B$ = 3.3 K/T decrease. The difference between the experimental value of dT_M/dB is −4.2 K/T and the calculated value is supposed to the latent heat of the first order martensite transformation.

Kataoka *et al.*, studied about the martensite transformation and ferromagnetic transition of $Ni_2Mn_{1-x}Cu_xGa$ ($0 \le x \le 0.40$) [31] and $Ni_2MnGa_{1-y}Cu_y$ ($0 \le x \le 0.40$) [48] alloys and made $x - T$, or $y - T$ phase diagrams. They suggested that the characteristics of the phase diagrams are very similar to those of Ni_{2+x} $Mn_{1-x}Ga$ ($0 \le x \le 0.40$) alloys [49]. Kataoka *et al.* [31] explained the phase diagram of $Ni_2Mn_{1-x}Cu_xGa$ ($0 \le x \le 0.40$) alloys using the Landau-type phenomenological free energy as a function of the martensitic distortion and magnetization. Their analysis showed that the bi-quadratic coupling term, together with a higher order term, of the martensitic distortion and magnetization plays an important role in the interplay between the martensite phase and the ferromagnetic phase. Their calculation based on the phenomenological free energy is shown as

$$F_{tot} = F_{ela} + F_{mag} + F_{mag\text{-}ela} \quad (6)$$

where, F_{tot} is the total free energy, F_{ela} the free energy of the elastic strain e_{ij}, F_{mag} the free energy of the magnetic system including the magnetic exchange energy and the magnetocrystalline anisotropy energy, and $F_{mag\text{-}ela}$ the energy of the interaction between the distortion and the magnetization. The calculated $x - T$ phase diagram of $Ni_2Mn_{1-x}Cu_xGa$ agrees well with the phase diagram, which was obtained from the experimental results. In addition, they suggested that the bi-quadratic term, $e_3^2M^2$, in $F_{mag\text{-}ela}$ affects the large magneto-structural coupling. Thus, strong magneto-structural coupling was displayed to play an important role in the magnetic properties and phase transitions of FSMAs. In the last part of Section 1,

we mentioned about the magnetocrystalline anisotropy. The large magnetocrystalline anisotropy influences the magneto-elastic coupling $F_{\text{mag-ela}}$ by means of the bi-quadratic term, $e_3^2 M^2$. In $Ni_{50-x}Co_xMn_{31.5}Ga_{18.5}$ ($0 \leq x \leq 9$), magnetization M increases with the magnetic field between 338 K and 388 K [41]. The thermal hysteresis of the thermal strain also decreases at high magnetic fields. Other Heusler compounds such as $Ni_{50+x}Mn_{12.5}Fe_{12.5}Ga_{25-x}$, show an x–T phase diagram similar to that of $Ni_2Mn_{1-x}Cu_xGa$ [20]. In comparison with the experimental results of $Ni_{41}Co_9Mn_{31.5}Ga_{18.5}$ and $Ni_2Mn_{1-x}Cu_xGa$, it is considered that the thermal hysteresis of the thermal strain that decreases with increasing magnetic field is an indication of strong magneto-structural coupling in $Ni_{41}Co_9Mn_{31.5}Ga_{18.5}$. The magnetic field-induced strain in single crystal, or magnetostriction in polycrystal in Ni_2MnGa, Ni-Co-Mn-Ga, and Ni-Co-Mn-In alloys also suggest a strong magneto-structural coupling. In the next section, we will mention the magnetic field-induced strains of the magnetic shape memory alloys.

3. Magnetic Field-Induced Strain and Magnetostriction in Shape Memory Alloys

Large magnetic field-induced strains (MFISs) have been observed in several Heusler single crystal alloys. These materials based on a Ni_2MnGa alloys have been characterized on the basis of the rearrangement of martensitic structural variants due to an external field [1,50,51]. MFISs of 6.0% have been produced at room temperature in single crystals of $Ni_{49.8}Mn_{28.5}Ga_{21.7}$ (T_M = 318 K) by application of fields of order 400 kA/m (=0.50 T) under an opposing stress of order 1 MPa [52]. The strain is the result of field-induced twin boundary motion. A disordered Fe-31.2%Pd (at.%) alloy (A1-type cubic) [53,54], and an ordered Fe_3Pt ($L1_2$-type cubic) ferromagnetic alloy [55,56], have attracted considerable interest due to the large MFISs. The Ni-Mn-Ga, Fe-Pd, and Fe-Pt alloy shave attracted considerable attention as materials for magnetic actuators. Recently, MFIS experiments at an AC magnetic field or pulse magnetic field have been carried out and the dynamical MFIS response of the Ni-Mn-Ga alloy has been reported by Henry *et al.* [57]. The 3% MFIS of FSMA $Ni_{49.8}Mn_{28.5}Ga_{21.7}$ at uniaxial bias stress of 1.6 MPa and an AC magnetic field of 2 Hz has been observed at the AC fields of 6 kOe. Even at a faster AC field, a strain of 2.5% at 150 Hz and a strain of 0.6% at 332 Hz have been observed. On the other hand, the MFISs without a bias stress have been observed in the Fe-Pd and Fe-Pt alloys. As for a Fe-31.2%Pd (at.%) single crystal alloy, a strain of 0.4% has been observed in single-shot pulse fields at the fields of 12 kOe with a frequency of 80 Hz at 77 K, which is much lower than the martensite transformation temperature T_M = 230 K [58]. With regard to the Fe_3Pt single crystal alloy, an MFIS of 1.7% has been observed and a recoverable strain of about 0.6% has been induced in single-shot pulse fields at the fields of 20 kOe with a frequency of 160 Hz at 4.2 K in the martensite state (T_M = 85 K) [59].

New alloys in the Ni-Mn-In, Ni-Mn-Sn, and Ni-Mn-Sb Heusler alloy systems, which are ferromagnetic shape memory alloys, have been studied by a Tohoku University group of researchers [60]. These alloys indicate a very small magnetization in the martensite phase compared to the parent phase. Oikawa *et al.* [61] studied the magnetic and martensite transformation behaviors of a $Ni_{46}Mn_{41}In_{13}$ alloy through various techniques, such as scanning calorimetry and vibrating sample magnetometry. A metamagnetic transition from the paramagnetic martensite phase to the ferromagnetic austenite phase was detected and a magnetic field-induced reverse martensite transformation was confirmed in a high magnetic field. This alloy is a metamagnetic shape memory alloy with a magnetic field-induced shape

memory effect and is used as a magnetocaloric material. Ni-Co-Mn-In alloys, in which Co is added to Ni-Mn-In to increase Curie temperature, show a basic shape memory behavior in a compression stress-strain measurement. As for $Ni_{45}Co_5Mn_{36.7}In_{13.3}$ (13.3In), which was mentioned in Section 2, a large MFIS has been observed [42]. After a compression prestrain of about 3% was applied to the 13.3In alloy, the steady magnetic field was applied parallel to the compression axis of the sample. The MFIS was measured by a three-terminal capacitance method. The expansion of 3% was observed at around 35 kOe, indicating an almost complete shape recovery induced by a magnetic field. Using this expansion, a stress of about 100 MPa was generated in the material on the application of a magnetic field. This stress level is about 50-fold higher than those of other shape memory alloys.

Polycrystal samples are better for magnetostriction measurements as MFIS is hindered by the grain boundaries [62]. Therefore, the realistic magnitude of the magnetostriction can be observed. Barandiarán *et al.* [62] observed the magnetostriction in polycrystal $Ni_{51.1}Mn_{24.9}Ga_{24.0}$. The sign of the longitudinal magnetostriction is negative and the magnitude is 100 ppm or smaller. The magnitude of the longitudinal magnetostriction at 1.5 T is −67 ppm at 180 K. The minus sign indicates the contraction. They mentioned that the observed behavior can only be understood if the short easy axes of tetragonal martensitic lattice (c-axis) are preferably aligned perpendicularly to the slab plane.

Sakon *et al.* [19] measured the strain for polycrystal $Ni_{52}Mn_{25}Ga_{23}$. At zero magnetic field, the strain is 3.6×10^{-4} (Figure 5). On the other hand, the strain in a magnetic field is about 7.1×10^{-4}, which is almost twice that in zero field. Ullakko *et al.* [1] measured the magnetic field-induced strain of a Ni_2MnGa single crystal. The strain at T_M in zero field was 2×10^{-4}. This is only a small fraction compared to the lattice constant change for *c*-axis from the austenite to martensite phase, which was $\Delta c/c = 6.56\%$. It is proposed that the strain accommodation occurs by different twin variant orientations. On the contrary, the thermal strain under the magnetic field of 5 T at 300 K in the ferromagnetic martensite phase was 720 ppm, indicating that the field aligned some of the twin variants. The magnetostriction at 300 K in the ferromagnetic martensite phase at 10 T is −100 ppm [19].

We discuss the difference of the driving forces of the variant rearrangements in two cases. One is martensitic transformation, shown in Figure 5, and the other is magnetostriction [19]. In the former case, the driving force is originated from phase transformation. Therefore, the magnitude is great and, as a consequence, the phase-induced variant rearrangements are easy and occur throughout the sample. For the latter case, the magnetic field-induced twin boundary motion is driven by the limited magnetic anisotropy energy, which is lower than the martensitic phase transformation driving force. Consequently, the variant orientation is limited by the mobile twin boundaries that are not pinned by any obstacles such as grain boundaries or defects. As a result, the variant rearrangement and magnetostriction are limited. Therefore, the magnetostriction is smaller than the strain at T_M in the linear strain measurements. The magnetostriction of the polycrystalline $Ni_{50}Mn_{28}Ga_{22}$ alloy was reported by Murray *et al.* [18]. They mentioned that the strain in the martensite phase below T_M is an order of magnitude smaller than that of a single crystal of the stoichiometric compounds [1]. They attributed this to the polycrystalline nature of the material or to the presence of impurities that impede twin boundary motion. The field-induced strain of $Ni_{50}Mn_{28}Ga_{22}$ increases on cooling from the austenite phase, leading to an abrupt increase with the appearance of the twin variant below T_M. On heating from the martensite phase, an abrupt increase occurs in the field-induced strain around T_M. They suggest that this is caused by lattice softening near T_M. As for the thermal strain of $Ni_{52}Mn_{25}Ga_{23}$, shown in Figure 5, peaks appear

for both T_M and T_R in zero field and all values of the magnetic field. The peak at T_R, associated with heating, is larger than that at T_M, associated with cooling. These peaks indicate that the lattice expands abruptly. Dai *et al.* [21] studied the elastic constants of a $Ni_{0.50}Mn_{0.284}Ga_{0.216}$ single crystal using the ultrasonic continuous-wave method. C_{11}, C_{33}, C_{66}, and C_{44} modes were investigated; every mode indicated abrupt softening around T_M. This lattice softening appears to be affected by the abrupt expansion just above T_M when cooling from the austenite phase. Barandiarán *et al.* [62] also suggest that physical reason of large variations at the martensite transformation temperatures is the lattice softening.

Now, we describe $Ni_{41}Co_9Mn_{31.5}Ga_{18.5}$ alloy, where the martensitic transformation and magnetic transition occur at the same temperature, T_M. Polycrystal $Ni_{41}Co_9Mn_{31.5}Ga_{18.5}$ shows the magnetostriction in steady magnetic fields [40]. When increasing the magnetic field, distinct magnetostriction was observed at the temperatures between T_M and T_R. The magnetic field dependences of magnetostriction and magnetization are shown in Figure 7. These measurements were performed after zero fields cooling to the temperature of 300 K in the paramagnetic martensite phase. The magnetization shows metamagnetic transition. The magnetostriction was also observed at the same temperature, 350 K. The metamagnetism and magnetostriction are due to the magnetic field-induced magnetic transition and martensite transformation from the paramagnetic martensite phase to the ferromagnetic austenite phase. The magnitude of the magnetostriction was 1.1×10^{-3} (0.11%) at maximum between 320 K and 360 K, which was approximately the same value as that of the thermal strain for the reverse martensite transformation. The magnitude of the magnetostriction of $Ni_{41}Co_9Mn_{31.5}Ga_{18.5}$ is 10 times larger than that of $Ni_{52}Mn_{25}Ga_{23}$. As for $Ni_{41}Co_9Mn_{31.5}Ga_{18.5}$, the metamagnetic transition and martensite transformation occurs simultaneously. Therefore, the magnitude is larger than the alloys, in which martensite transformation occurs in a ferromagnetic phase.

Previous MFIS measurements performed for 13.3In were under a compressive pre-strain of 100 MPa. However, the magnetostriction measurements in this study were performed under atmospheric pressure and without the compression pre-strain. The *M-B* curves and the thermal strain suggest that the magneto-structural transition of $Ni_{41}Co_9Mn_{31.5}Ga_{18.5}$ alloy is sensitive to magnetic fields. The magnitude of the magnetic field strains and the magnetostrictions of the magnetic shape memory alloys are shown in Table 3.

Table 3. The magnetic field induced strains and the magnetostrictions of shape memory alloys.

Sample	Crystal structure	crystalline	Magnitude	Remarks
$Ni_{49.8}Mn_{28.5}Ga_{21.7}$	$Fm\bar{3}m$	Single	6.0% at 300 K under 1 MPa	[52]
Fe-31.2%Pd (at.%)	Disordered A1	Single	3.0% at 4.2 K	[53,54]
Fe_3Pt	$L1_2$	Single	2.3% at 4.2 K	[55,56]
$Ni_{45}Co_5Mn_{36.7}In_{13.3}$	14M	Single	3.0% at 298 K	[42]
$Ni_{51.1}Mn_{24.9}Ga_{24.0}$	$D0_{22}$	Poly	−67 ppm at 180 K	[62]
$Ni_{52}Mn_{25}Ga_{23}$	14M	Poly	−100 ppm at 300 K	[19]
$Ni_{41}Co_9Mn_{31.5}Ga_{18.5}$	$D0_{22}$	Poly	0.11% at 350 K	[40]

Figure 7. The magnetic field dependence of the magnetostriction and magnetization of polycrystal $Ni_{41}Co_9Mn_{31.5}Ga_{18.5}$ at the temperatures between T_M and T_R.

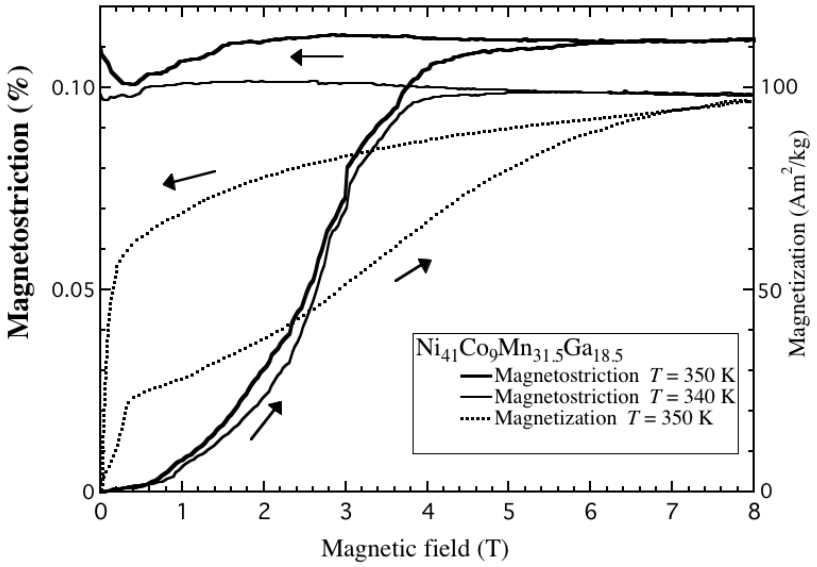

Finally, we introduce a new measurement system for the magnetostriction or magnetic transformation in pulse magnetic fields. An *in situ* microscopic imaging observation system has been developed by Xu *et al.* [63], and it was performed on $Ni_{45}Co_5Mn_{36.7}In_{13.3}$ metamagnetic shape memory alloy in pulse magnetic fields (time constant is 4.6 ms). Magnetic field-induced reverse martensitic transformation and heating-induced martensitic transformation were directly observed by means of an optical microscope between 8.5 K and 180 K with a maximum field of 31 T. A fraction of the martensite phase was evaluated by contrast change from micrographs and critical magnetic fields were determined. Isothermal growth of martensite after magnetic field application was also clearly observed. Comparison between the micrographs after the application of a magnetic field and on cooling also revealed the nature of the adiabatic process under a strong driving force.

In the last part of the reference lists in this paper, some papers concerning to the magnetic shape memory alloys are listed denoted by A to C sign. A: Magnetic field influence on martensite transformation in ferromagnetic shape memory alloys and metamagnetic shape memory alloys [64–70]; B: Magnetic anisotropy of the ferromagnetic shape memory alloys [71,72]; C: Magnetostriction [73,74].

4. Summary

Magneto-structural properties of novel Ni_2MnGa type FSMAs in magnetic fields were introduced. These alloys indicate large magnetic field dependence of dT_M/dB or dT_R/dB when the martensite transformation (or reverse martensite transformation) and magnetic phase transition occur at the same temperature. A consideration by means of the phenomenological analysis by Satyanarayan *et al.* [46] and Nishiyama [47] was performed and it was explained that the Heusler alloys, which show re-entrant magnetism (high temperature phase: ferromagnetic austenite; low temperature phase: paramagnetic martensite), the sign of dT_M/dB or dT_R/dB is negative. Giant magnetic field-induced strain was determined with some novel alloys. Novel measurement system for investigation of the MFIS was also introduced.

Acknowledgments

This study was supported by a Grant-in-Aid for Scientific Research (C) (Grant No. 24560798) from the Japan Society for the Promotion of Science (JSPS) of the Ministry of Education, Culture, Sports, Science and Technology, Japan.

References

1. Ullakko, K.; Huang, J.K.; Kantner, C.; O'Handley, R.C.; Kokorin, V.V. Large magnetic-field-induced strains in Ni_2MnGa single crystals. *Appl. Phys. Lett*. **1996**, *69*, 1966–1968.
2. Webster, P.J.; Ziebeck, K.R.A.; Town, S.L.; Peak, M.S. Magnetic order and phase transformation in Ni_2MnGa. *Philos. Mag. B* **1984**, *49*, 295–310.
3. Brown, P.J.; Crangle, J.; Kanomata, T.; Matsumoto, M.; Neumann, K-.U.; Ouladdiaf, B.; Ziebeck, K.R.A. The crystal structure and phase transitions of the magnetic shape memory compound Ni_2MnGa. *J. Phys. Condens. Matter.* **2002**, *14*, 10159–10171.
4. Pons, J.; Santamarta, R.; Chernenko, V.A.; Cesari, E. Long-Period martensitic structures of Ni-Mn-Ga alloys studied by high-resolution transmission electron microscopy. *J. Appl. Phys*. **2005**, *97*, 083516:1–083516:7.
5. Ranjan, R.; Banik, S.; Barman, S.R.; Kumar, U.; Mukhopadhyay, P.K.; Pandey, D. Powder x-ray diffraction study of the thermoelastic martensite transition in $Ni_2Mn_{1.05}Ga_{0.95}$. *Phys. Rev. B* **2006**, *74*, 224443:1-224443:2.
6. Jiang, C.; Feng, G.; Gong, S.; Xu, H. Effect of Ni excess on phase transformation temperatures of NiMnGa alloys. *Mater. Sci. Eng. A* **2003**, *342*, 231–235.
7. Ma, Y.; Jiang, C.; Li, Y.; Xu, H.; Wang, C.; Liu, X. Study of $Ni_{50+x}Mn_{25}Ga_{25-x}$ (x = 2–11) as high-temperature shape-memory alloys. *Acta Mater.* **2007**, *55*, 1533–1541.
8. Mañosa, L.; Moya, X.; Planes, A.; Krenke, T.; Acet, M.; Wassermann, E.F. Ni-Mn-based magnetic shape memory alloys: Magnetic properties and martensite transformation. *Mater. Sci. Eng. A* **2008**, *481–482*, 49–56.
9. Sánchez-Alarcos, V.; Pérez-Landazábal, J.I.; Gómez-Polo, C.; Recarte, V. Influence of the atomic order on the magnetic characteristics of a Ni–Mn–Ga ferromagnetic shape memory alloy. *J. Magn. Magn. Mater.* **2008**, *320*, e160–e163.
10. Rudajevová, A. Analysis of the thermal expansion characteristics of $Ni_{53.6}Mn_{27.1}Ga_{19.3}$ alloy. *J. Alloys Compd.* **2007**, *430*, 153–157.
11. Zhu, F.Q.; Yang, F.Y.; Chien, C.L.; Ritchie, L.; Xiao, G.; Wu, G.H. Magnetic and thermal properties of Ni–Mn–Ga shape memory alloy with Martensite transition near room temperature. *J. Magn. Magn. Mater.* **2005**, *288*, 79–83.
12. Chernenko, V.A.; L'vov, V.A.; Khovailo, V.V.; Takagi, T.; Kanomata, T.; Suzuki, T.; Kainuma, R. Interdependence between the magnetic properties and lattice parameters of Ni–Mn–Ga martensite. *J. Phys. Condens. Matter*. **2004**, *16*, 8345–8352.
13. Golub, V.O.; Vovk, A.Y.; O'Connor, C.J.; Kotov, V.V.; Yakovenko, P.G.; Ullakko, K. Magnetic and structural properties of nonstoichiometric Ni_2MnGa alloys with Ni and Ga excess. *J. Appl. Phys.* **2003**, *93*, 8504–8506.

14. Kim, J.; Inaba, F.; Fukuda, T.; Kakeshita, T. Effect of magnetic field on martensitic transformation temperature in Ni–Mn–Ga ferromagnetic shape memory alloys. *Acta Mater.* **2006**, *54*, 493–499.
15. González-Comas, A.; Obradó, E.; Mafiosa, L.; Planes, A.; Labarta, A. Magnetoelasticity in the Heusler Ni_2MnGa alloy. *J. Magn. Magn. Mater*. **1999**, *196–197*, 637–638.
16. Lanska, N.; Söderberg, O.; Sozinov, A.; Ge, Y.; Ullakko, K.; Lindroos, V.K. Composition and temperature dependence of the crystal structure of Ni–Mn–Ga alloys. *J. Appl. Phys*. **2004**, *95*, 8074–8078.
17. Likhachev, A.A.; Ullakko, K. Magnetic-field-controlled twin boundaries motion and giant magneto-mechanical effects in Ni–Mn–Ga shape memory alloy. *Phys. Lett. A* **2000**, *275*, 142–151.
18. Murray, S.J.; Farinelli, M.; Kantner, C.; Huang, J.K.; Allen, S.M.; O'Handley, R.C. Field-induced strain under load in Ni–Mn–Ga magnetic shape memory materials. *J. Appl. Phys*. **1998**, *83*, 7297–7299.
19. Sakon, T.; Nagashio, H.; Sasaki, K.; Susuga, S.; Numakura, D.; Abe, M.; Endo, K.; Yamashita, S.; Nojiri, H.; Kanomata, T. Thermal strain and magnetization of the ferromagnetic shape memory alloy $Ni_{52}Mn_{25}Ga_{23}$ in a magnetic field. *J. Phys. Chem. Solids* **2013**, *74*, 158–165.
20. Kikuchi, D.; Kanomata, T.; Yamaguchi, Y.; Nishihara, H. Magnetic properties of ferromagnetic shape memory alloys $Ni_{50+x}Mn_{12.5}Fe_{12.5}Ga_{25-x}$. *J. Alloys Compd*. **2006**, *426*, 223–227.
21. Dai, L.; Cullen, J.; Wuttig, M. Intermartensitic transformation in a NiMnGa alloy. *J. Appl. Phys*. **2004**, *95*, 6957–6959.
22. Straka, L.; Heczko, O. Magnetic anisotropy in Ni-Mn-Ga martensite, *J. Appl. Phys*. **2003**, *93*, 8636–8638.
23. Callen, H.B.; Callen, E. The present status of the temperature dependence of magnetocrystalline anisotropy, and the $l(l+1)/2$ power law. *J. Phys. Chem. Solids* **1966**, *27*, 1271–1285.
24. Ziljistra, H. *Experimental Methods in Magnetism 2*; North-Holland Pub. Co.: Amsterdam, The Neatherland, 1967; pp. 168–181.
25. Graham, C.D., Jr. Magnetocrystalline anisotropy constants of iron at room temperature and below. *Phys. Rev.* **1958**, *112*, 1117–1120.
26. Okamoto, N.; Fukuda, T.; Kakeshita, T.; Takeuchi, T. Magnetocrystalline anisotropy constant and twinning stress in martensite phase of Ni–Mn–Ga. *Mat. Sci. Eng. A* **2006**, *438–440*, 948–951.
27. Heczko, O.; Straka, L.; Novak, V.; Fähler, S. Magnetic anisotropy of nonmodulated Ni–Mn–Ga martensite revisited. *J. Appl. Phys.* **2010**, *107*, 09A914:1–09A914:3.
28. Koyama, K.; Fujii, H.; Canfield, P.C. Magnetocrystalline anisotropy of a Nd_2Fe_{17} single crystal. *Physica. B* **1996**, *226*, 363–369.
29. Sakon, T.; Saito, S.; Koyama, K.; Awaji, S.; Sato, I.; Nojima, T.; Watanabe, K.; Sato, N.K. Experimental investigation of giant magnetocrystalline anisotropy of UGe_2. *Phys. Scr*. **2007**, *75*, 546–550.
30. Boulet, P.; Daoudi, A.; Potel, M.; Noël, M.; Gross, G.M.; André, G.; Bourée, F. Crystal and magnetic structure of the uranium digermanide UGe_2. *J. Alloys Comp*. **1997**, *247*, 104–108.
31. Kataoka, M.; Endo, K.; Kudo, N.; Kanomata, T.; Nishihara, H.; Shishido, T.; Umetsu, R.Y.; Nagasako, M.; Kainuma, R. Martensitic transformation, ferromagnetic transition, and their interplay in the shape memory alloys $Ni_2Mn_{1-x}Cu_xGa$. *Phys. Rev. B* **2010**, *82*, 1–14.

32. Oikawa, K.; Ota, T.; Ohmori, T.; Tanaka, Y.; Morito, H.; Fujita, A.; Kainuma, R.; Fukamichi, K.; Ishida, K. Magnetic and martensitic phase transitions in ferromagnetic Ni–Ga–Fe shape memory alloys. *Appl. Phys. Lett*. **2002**, *81*, 5201–5203.
33. Sutou, Y.; Kamiya, N.; Omori, T.; Kainuma, R.; Ishida, K.; Oikawa, K. Stress-strain characteristics in Ni–Ga–Fe ferromagnetic shape memory alloys. *Appl. Phys. Lett*. **2004**, *84*, 1275–1277.
34. Oikawa, K.; Ota, T.; Sutou, Y.; Ohmori, T.; Kainuma, R.; Ishida, K. Magnetic and martensitic phase transformations in a $Ni_{54}Ga_{27}Fe_{19}$ Alloy. *Mater. Trans*. **2002**, *43*, 2360–2362.
35. Sakon, T.; Nagashio, H.; Sasaki, K.; Susuga, S.; Endo, K.; Nojiri, H.; Kanomata, T. Thermal expansion and magnetization studies of novel ferromagnetic shape memory alloys $Ni_{52}Mn_{12.5}Fe_{12.5}Ga_{23}$ and $Ni_2Mn_{0.75}Cu_{0.25}Ga$. *Mater. Trans*. **2011**, *52*, 1142–1147.
36. Vasil'ev, A.N.; Estrin, E.I.; Khovailo, V.V.; Bozhko, A.D.; Ischuk, R.A.; Matsumoto, M.; Takagi, T.; Tani, J. Dilatometric study of $Ni_{2+x}Mn_{1-x}Ga$ under magnetic field. *Int. Appl. Electromagn. Mechan*. **2000**, *12*, 35–40.
37. Kikuchi, D. Thermomagnetic Properties of Quarternary Ni-Mn-Fe-Ga Ferromagnet Shape Memory Alloys. Master Thesis, Tohoku Gakuin University, Takajo, Japan, 2005.
38. Sakon, T.; Nagashio, H.; Sasaki, K.; Susuga, S.; Numakura, D.; Abe, M.; Endo, K.; Nojiri, H.; Kanomata, T. Thermal expansion and magnetization studies of the novel ferromagnetic shape memory alloy $Ni_2MnGa_{0.88}Cu_{0.12}$ in a magnetic field. *Physica Scripta* **2011**, *84*, 1–6.
39. Albertini, F.; Fabbrici, S.; Paoluzi, A.; Kamarad, J.; Arnold, Z.; Righi, L.; Solzi, M.; Porcari, G.; Pernechele, C.; Serrate, D.; *et al*. Reverse magnetostructural transitions by Co and In doping NiMnGa alloys: Structural, magnetic, and magnetoelastic properties. *Mater. Sci. Forum* **2011**, *684*, 151–163.
40. Sakon, T.; Sasaki, K.; Numakura, D.; Abe, M.; Nojiri, H.; Adachi, Y.; Kanomata, T. Magnetic field-induced transition in Co-Doped $Ni_{41}Co_9Mn_{31.5}Ga_{18.5}$ Heusler Alloy. *Mater. Trans*. **2013**, *54*, 9–13.
41. Sakon, T.; Nojiri, H.; Adachi, Y.; Kanomata, T. Crystallography and Magnetic field-induced strain by Co doping NiCoMnGa Heusler alloy. *TMS2013 Suppl. Proc.* **2013**, doi:10.1002/9781118663547.ch120.
42. Kainuma, R.; Imano, Y.; Ito, W.; Sutou, Y.; Morino, H.; Okamoto, S.; Kitakami, O.; Oikawa, K.; Fujita, A.; Kanomata, T.; *et al*. Magnetic-field-induced shape recovery by reverse phase transformation. *Nature* **2006**, *439*, 957–960.
43. Monroe, J.A.; Karaman, I.; Basaran, B.; Xu, X.; Ito, W.; Umetsu, R.Y.; Kainuma, R.; Koyama, K.; Chumlyakov, Y.I. Kinetic arrest of martensitic transformation in $Ni_{33.0}Co_{13.4}Mn_{39.7}Ga_{13.9}$ metamagnetic shape memory alloy. *Mater. Trans*. **2010**, *51*, 469-471.
44. Sakon, T.; Yamazaki, S.; Kodama, Y.; Motokawa, M.; Kanomata, T.; Oikawa, K.; Kainuma, R.; Ishida, K. Magnetic field-induced strain of Ni–Co–Mn–In alloy in pulsed magnetic field. *Jpn. J. Appl. Phys*. **2007**, *46*, 995–998.
45. Casanova, F.; Battle, X.; Labarta, A.; Marcos, J.; Manósa, L.; Planes, A. Entropy change and magnetocaloric effect in $Gd_5(Si_xGe_{1-x})_4$. *Phys. Rev. B* **2002**, *66*, 100401:1–100401:4.
46. Satyanarayan, K.R.; Eliasz, W.; Miodownik, A.P. The effect of a magnetic field on the martensite transformation in steels. *Acta Metall*. **1968**, *16*, 877–887.

47. Nishiyama, Z.; Fine, M.E.; Meshii, M.; Wayman, C.M. *Martensite Transformation*; Academic Press: Tokyo, Japan, 1971.
48. Kanomata, T.; Endo, K.; Kudo, N.; Umetsu, R.Y.; Nishihara, H.; Kataoka, M.; Nagasako, M.; Kainuma, R.; Ziebeck, K.R.A. Magnetic moment of Cu-modified Ni_2MnGa magnetic shape memory alloys. *Metals* **2013**, *3*, 114–122.
49. Khovaylo, V.V.; Buchelnikov, V.D.; Kainuma, R.; Koledov, V.V.; Ohtsuka, M.; Shavrov, V.G.; Takagi, T.; Taskaev, S.V.; Vasiliev, A.N. Phase transitions in $Ni_{2+x}Mn_{1-x}Ga$ with a high Ni excess. *Phys. Rev. B* **2005**, *72*, 224408:1–224408:10.
50. Ullakko, K.; Huang, J.K.; Kokorin, V.V.; O'Handley, R.C. Magnetically controlled shape memory effect in Ni_2MnGa intermetallics. *Scr. Mater*. **1997**, *36*, 1133–1138.
51. Kakeshita, T.; Ullakko, K. Giant magnetostriction in ferromagnetic shape-memory alloys. *MRS Bull.* **2002**, *27*, 105–109.
52. Murray, S.J.; Marioni, M.; Allen, S.M.; O'Handley, R.C. 6% magnetic-field-induced strain by twin-boundary motion in ferromagnetic Ni–Mn–Ga. *Appl. Phys. Lett.* **2000**, *77*, 886–888.
53. Kakeshita, T.; Fukuda, T.; Sakamoto, T.; Takeuchi, T.; Kindo, K.; Endo, S.; Kishino, K. Martensitic transformation in shape memory alloys under magnetic field and hydrostatic pressure. *Mater. Trans.* **2002**, *43*, 887–892.
54. Sakamoto, T.; Fukuda, T.; Kakeshita, T.; Takeuchi, T.; Kishino, K. Magnetic field-induced strain in iron-based ferromagnetic shape memory alloys. *J. Appl. Phys*. **2003**, *93*, 8647.
55. Kakeshita, T.; Fukuda, T. Conversion of variants by magnetic field in Iron-based ferromagnetic shape memory alloys. *Mater. Sci. Forum* **2003**, *426–432*, 2309–2314.
56. Fukuda, T.; Sakomoto, T.; Inoue, T.; Kakeshita, T.; Kishio, K. Influence of magnetic field direction on recoverable strain due to rearrangement of variants in Fe_3Pt. *Trans. Mater. Res. Soc. Jpn*. **2004**, *29*, 3059–3060.
57. Henry, C.P.; Feuchtwanger, J.; Bono, D.; O'Handley, R.C.; Allen, A.M. Dynamic Magnetic Field-Induced Strain Response of $Ni_{49.8}Mn_{28.5}Ga_{21.7}$ Ferromagnetic Shape Memory Alloy up to 332 Hz. In *The Fourth Pacific Rim International Conference. Advanced Materials and Processing (PRICM4)*, Hawaii, USA, 11–15 December, 2001; pp. 1657–1660.
58. Sakon, T.; Takaha, A.; Matsuoka, Y.; Obara, K.; Saito, T.; Motokawa, M.; Fukuda, T.; Kakeshita, T. Field-induced strain of shape memory alloy Fe-31.2%Pd using a capacitance method in a pulsed magnetic field. *Jpn. J. Appl. Phys*. **2004**, *43*, 7467–7471.
59. Sakon, T.; Takaha, A.; Obara, K.; Dejima, K.; Nojiri, H.; Motokawa, M.; Fukuda, T.; Kakeshita, T. Magnetic-field-induced strain of shape-memory alloy Fe_3Pt studied by a capacitance method in a pulsed magnetic field. *Jpn. J. Appl. Phys*. **2007**, *46*, 146–151.
60. Sutou, Y.; Imano, Y.; Koeda, N.; Omori, T.; Kainuma, R.; Ishida, K.; Oikawa, K. Magnetic and martensitic transformations of NiMnX (X = In, Sn, Sb) ferromagnetic shape memory alloys. *Appl. Phys. Lett.* **2004**, *85*, 4358–4360.
61. Oikawa, K.; Ito, W.; Imano, Y.; Sutou, Y.; Kainuma, R.; Ishida, K.; Okamoto, S.; Kitakami, O.; Kanomata, T. Effect of magnetic field on martensite transformation of $Ni_{46}Mn_{41}In_{13}$ Heusler alloy. *Appl. Phys. Lett.* **2006**, *88*, 122507:1–122507:3.
62. Barandiarán, J.M.; Chernenko, V.A.; Gutiérrez, J.; Orúe, I.; Lázpita, P. Magnetostriction in the vicinity of structural transitions in Ni_2MnGa. *Appl. Phys. Lett.* **2012**, *100*, 262410:1–262410:5.

63. Xu, X.; Ito, W.; Katakura, I.; Tokunaga, M.; Kainuma, R. *In situ* optical microscopic observation of NiCoMnIn metamagnetic shape memory alloy under pulsed high magnetic field. *Scr. Mater.* **2011**, *65*, 946–949.
64. Barandiarán, J.M.; Chernenko, V.A.; Cesari, E.; Salas, D.; Lazpita, P.; Gutierrez, J.; Orue, I. Magnetic influence on the martensitic transformation entropy in Ni-Mn-In metamagnetic alloy. *Appl. Phys. Lett.* **2013**, *102*, 071904:1–071904:4.
65. Entel, P.; Siewert, M.; Gruner, M.E.; Herper, H.C.; Comtesse, D.; Arroyave, R.; Singh, N.; Talapatra, A.; Sokolovskiy, V.V.; Buchelnikov, V.D.; *et al*. Complex magnetic ordering as a driving mechanism of multifunctional properties of Heusler alloys from first principles. *Eur. Phys. J. B* **2013**, *86*, 65:1–65:11.
66. Lázpita, P.; Barandiarán, J.M.; Gutiérrez, J.; Feuchtwanger, J.; Chernenko, V.A.; Richard, M.L. Magnetic moment and chemical order in off-stoichiometric Ni-Mn-Ga ferromagnetic shape memory alloys. *N. J. Phys.* **2011**, *13*, 033039:1–033039:14.
67. Lázpita, P.; Chernenko, V.A.; Barandiarán, J.M.; Orue, I.; Gutiérrez, J.; Feuchtwanger, J.; Rodriguez-Velamazán, J.A. Influence of magnetic field on magnetostructural transition in $Ni_{46.4}Mn_{32.8}Sn_{20.8}$ Heusler alloy. *Mater. Sci. Forum* **2010**, *635*, 89–95.
68. Barandiarán, J.M.; Chernenko, V.A.; Lázpita, P.; Gutiérrez, J.; Feuchtwanger, J. Effect of martensitic transformation and magnetic field on transport properties of Ni-Mn-Ga and Ni-Fe-Ga Heusler alloys. *Phys. Rev. B* **2009**, *80*, 104404:1–104404:7.
69. Chernenko, V.A.; Lv'ov, V.A. ; Kanomata, T.; Kakeshita, T.; Koyama, K.; Besseghini, S. Martensitic transformation in Ni-Mn-Ga alloy under high magnetic fields. *Mater. Trans.* **2006**, *47*, 635–638.
70. Oikawa, K.; Imano, Y.; Chernenko, V.A.; Luo, F.; Omori, T.; Sutou, Y.; Kainuma, R.; Kanomata, T.; Ishida, K. Influence of Co addition on martensitic and magnetic transitions in Ni-Fe-Ga β based shape memory alloys. *Mater. Trans.* **2005**, *46*, 734–737.
71. Chernenko, V.A.; L'vov, V.A.; Golub, V.; Aseguinolaza, I.R.; Barandiarán, J.M. Magnetic anisotropy of mesoscale-twinned Ni-Mn-Ga thin films. *Phys. Rev. B* **2011**, *84*, 054450:1–054450:7.
72. L'vov, V.; Chernenko, V. Magnetic anisotropy of ferromagnetic martensites. *Mater. Sci. Forum* **2011**, *684*, 31–47.
73. Chernenko, V.A.; L'vov, V.A. Magnetoelastic nature of ferromagnetic shape memory effect. *Mater. Sci. Forum* **2008**, *583*, 1–20.
74. L'vov, V.; Zagorodnyuk, S.; Chernenko, V.; Takagi, T. Magnetic-field-induced stresses and magnetostrain effect in martensite. *Mater. Trans.* **2002**, *43*, 876–880.